PHYSICAL REVIEW B VOLUME 46, NUMBER 18 1 NOVEMBER 1992-II

Glass transition on long time scales

R. Brüning and K. Samwer
Institut für Physik, Universität Augsburg, Memminger Strasse 6, 8900 Augsburg, Germany

(Received 19 June 1992)

Calorimetric measurements of the glass transition are presented for metallic glasses, B_2O_3, and organic polymers with cooling and heating rates ranging over more than three orders of magnitude. Fits of the onset temperatures of the glass transition to a Vogel-Fulcher-type equation give divergence temperatures significantly above the values obtained for Vogel-Fulcher fits to the viscosity. The width of the glass transition extrapolates to a sharp step transition at a finite heating and cooling rate, which is close to the range where the data were taken. The results suggest that the glass transition becomes independent of the experimental time scale in a regime that may be accessible to measurements.

INTRODUCTION

Although the glass transition has been studied for many decades, there is still an ongoing discussion about the basic nature of the phenomenon.[1-3] The viscosity of glass-forming systems changes dramatically near the glass transition. As a consequence, the time scale of the measurement determines where the characteristic changes occur which mark the transition to the glass. In particular, previously published calorimetric and volumetric experiments show a linear dependence of the glass-transition temperature, T_G, on the logarithm of the heating rate.[1,4-6] The glass transition may also be observed by scanning a probe frequency isothermally.[7,8] These experiments also show a decrease of T_G with the logarithm of the frequency. Based on these experimental observations no lower limit for T_G seems to exist, although it must be remembered that the time required for the observation of the glass transition at lower temperatures grows exponentially. However, some measurements indicate that an even stronger divergence at a nonzero temperature underlies the glass transition: (1) The viscosity of most glasses may be described by a Vogel-Fulcher form with a divergence at a temperature T_0.[1,2,9,10] However, the extrapolated divergence lies well below the observed glass transition (typically by 20–30 %). (2) The specific heat of the supercooled liquid is larger than the specific heat of the corresponding crystalline phases. Kauzmann observed that this difference is so large that the extrapolated entropy of the supercooled liquid becomes smaller than the entropy of the corresponding crystalline phases at an isentropic temperature, T_K.[11] Since in most cases that is physically unreasonable, the system must either crystallize or form a glass above T_K. The integration of data for the difference in specific heat between supercooled and crystallized $Pd_{40}Ni_{40}P_{20}$ (Ref. 12) gives $T_K=(517\pm8)$ K, which is 8% below the calorimetrically observed glass-transition temperature. (3) The attempt to analyze the dependence of T_G on the heating rate as the result of an activated process leads to activation energies which are a factor of 3 larger than the values found by diffusion measurements in the same temperature regime.[4,6,13] Even more striking is the inconsistency of the frequency prefactors, for which one finds values of 10^{30} Hz and higher.[13] A simple picture of activated processes fails to describe the glass transition and some cooperative effect appears to be underlying it.

These observations can be understood with the assumption that a temperature T_G^0 is a lower limit for T_G. T_G^0 should be close to, but in general above, T_K. To observe the effects of such a transition, it is necessary to measure glass formation on long time scales. In the present study, calorimetric measurements of the glass transition have been extended to comparatively low heating and cooling rates. Several systems of different types are included in this study: metallic glasses which are very stable against crystallization, organic polymers, and the inorganic polymer B_2O_3.

EXPERIMENTAL METHOD

The metallic glasses $Pd_{40}Ni_{40}P_{19}Si_1$, $Pd_{77.5}Si_{16.5}Ag_6$, and $La_{55}Al_{25}Ni_{20}$ were prepared by the conventional technique of melt spinning onto a copper wheel. The organic polymers are secondary standards of polymethylmethacrylate (PMMA, M.W. 93300, and M.N. 46400) and polycarbonate resin (PCR, M.W. 47900, and M.N. 18100) were purchased from Aldrich Chemicals, Inc., and were measured as received. Two samples of B_2O_3 were measured which contained different amounts of water. It was determined by weighing a series of dried samples that T_G decreases by 19 K per mol % of H_2O dissolved in B_2O_3. One sample was dried at 823 K for 1 h, and retained less than 0.1 mol % of water. A second sample of B_2O_3 was dried at 673 K for 10 min and retained about 2.7 mol % of water. The specific heat measurements were carried out with a differential scanning calorimeter (Perkin-Elmer DSC 7). The samples, apart from B_2O_3, were enclosed in air-tight aluminum pans. In the case of B_2O_3 small holes were punched into the lid of the sample pan so that the water could escape while the sample was dryed. A constant flow of argon was maintained in the instrument, except in the case of the measurements on $Pd_{40}Ni_{40}P_{19}Si_1$ where the gas flow was shut off after placing the sample inside and initially flushing the instrument with argon. The basic calibration of the instrument was done at a heating rate of 10 K/min with In and Zn melting point standards (429.4 and 692.7 K). As the exact calibration of the instrument depends on the heating rate, an additional temperature correction was determined for each heating rate, φ. Depending on which melting point lies closer to T_G of the sample to be measured, either an In or a Pb melting point standard (606.6 K) were used to determine this correction. The changes of the corrections with heating rate were typically 0 K for $\varphi < 1$ K/min, and 0.1, 0.2, 0.7, 1.2, 2.5, 5.5, 10.9, and 16.0 K for $\varphi = 1$, 2, 5, 10, 20, 50, 100, and 200 K/min. The corrections varied slightly with time and between the two standards, and were much smaller than the net shifts in T_G (typically 40 K). To increase the signal, relatively large amounts of sample were used for the measurements at low heating rates (for example, 119 mg for the measurements on $Pd_{40}Ni_{40}$ $P_{19}Si_1$). For the metallic samples, the amount of sample had little influence on the results of the measurements. A repetition of the measurement with a mass of 12 mg gave similar results, and it was only at the highest heating rate of 200 K/min that a shift of T_G by 2.5 K was seen. Apart from this small correction, all measurements for each metallic glass could be made on one sample. The samples were placed into the calorimeter and measured by repeatedly heating and cooling them through the glass transition. The measurements at different heating rates were done in a random sequence. For measurements on polymers, data from samples of different masses had to be combined because the thermal gradients within samples were too large for samples of large mass at high heating rates. All data was rejected for which a variation of the sample mass by a factor of 5 lead to a change in the value of T_G or a change in the shape of the calorimetric signal. For the polymers PMMA and PCR consistent data could only be obtained for heating rates up to 100 K/min or 20 K/min, respectively. A parabola was subtracted from the heat flow signals to correct for the variation of the baseline of the instrument with different heating rates. To obtain the changes in the specific heat, ΔC_P, the heat flow signals were then divided by φ.

RESULTS AND DISCUSSION

The samples are heated from the initial state to above the glass transition. Above T_G the systems are in the supercooled liquid state and in metastable equilibrium:[12] the state depends only on the temperature and not on the thermal history, i.e., the system is in equilibrium with respect to to all liquid states, but metastable with respect to crystallization. Then the samples are cooled to low temperatures with a rate $-\varphi$. On cooling a glass is formed which in general is out of equilibrium, and whose state depends on the cooling rate,[12] provided that the glass is cooled to a temperature which is low enough to avoid further relaxation below T_G. Subsequently, the sample is heated with the same rate φ to measure the transition upon heating. At the beginning and at the end of the cooling-heating cycle the sample is in metastable equilibrium above T_G. Since the cooling rate equals the heating rate, the evolution of the sample is tested only on a single time scale corresponding to $|\varphi|$. This cycle is repeated with $|\varphi|$ ranging from 0.1 to 200 K/min. Figure 1 shows the change of the specific heat during heating and cooling for $Pd_{40}Ni_{40}P_{19}Si_1$. Figures 2 and 3 show ΔC_P upon heating for $Pd_{40}Ni_{40}P_{19}Si_1$ and B_2O_3. The signature of the glass transition upon cooling is a decrease in ΔC_P over a range of about 50 K. During the subsequent heating there is a pronounced overshoot in the specific heat which occurs when the kinetics become fast enough to allow the sample to regain metastable equilibrium on the time scale of the measurement. The onset of the ΔC_P peak upon heating is the most pronounced feature of the transition and it is used here to identify T_G. It is defined as the point of intersection between the linearly extrapolated curve below the transition with the steepest tangent of the rise in ΔC_P. The onsets of the glass transition in $Pd_{40}Ni_{40}P_{19}Si_1$ are plotted in Figure 4 against the heating rate on a logarithmic scale. (Note that from now on the heating rate is given in K/s rather than in the experimentally practical unit K/min.) Clearly, the data points deviate from a straight line. This differs from the results that were reported previously.[4–6] It is apparent that the extension of the measurements to low heating rates is necessary to observe the deviation from a straight line in the semilogarithmic plot. This result is consistent with results of isothermal Mössbauer spectroscopy measurements of the Debye-Waller factor, which give a higher value of T_G than the extrapolated scanning calorimetry data.[13,14]

With respect to the discussion concerning a possible lower limit for the glass transition, it is of interest to see whether and how the values of T_G converge to some finite value T_G^0. To test this, one has to choose a function to compare the data with. It is standard procedure to fit viscosity measurements to a Vogel-Fulcher equation or a similar function.[9,10] A functional form of Vogel-Fulcher type which is suitable to fit the present results is

$$\varphi = B \exp[A/(T_G^0 - T_G)] \Longleftrightarrow T_G = T_G^0 + A/\ln(B/\varphi) \quad (1)$$

with $0 \le \varphi < B$. The adjustable parameters of such a fit

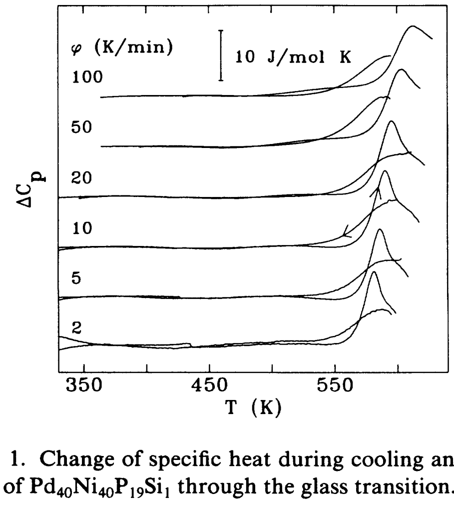

FIG. 1. Change of specific heat during cooling and heating a sample of $Pd_{40}Ni_{40}P_{19}Si_1$ through the glass transition.

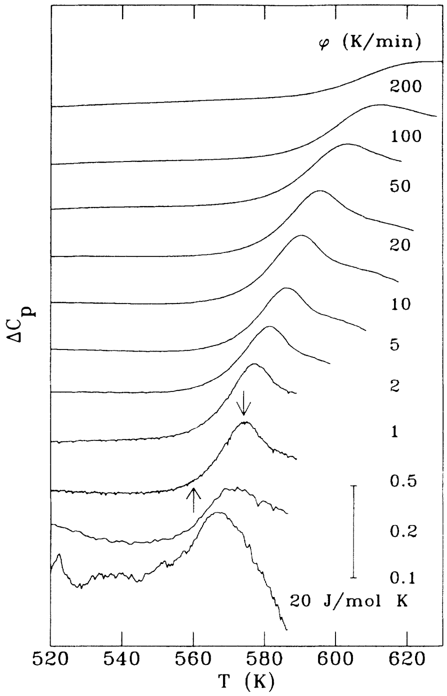

FIG. 2. Change of the specific heat at the glass transition of $Pd_{40}Ni_{40}P_{19}Si_1$ upon heating with rates φ varying between 0.1 and 200 K/min. Before heating the sample was cooled through the glass transition with the rate $-\varphi$.

are A, B, and T_G^0. The temperature T_G^0 is the asymptotic value of T_G in the limit of infinitely slow cooling and heating. B has the dimensions of a heating rate. The numerical values obtained for B are so far above the highest heating rates used that the unphysical divergence of the fitting function at $\varphi \rightarrow B$ can be disregarded for the following discussion. For $Pd_{40}Ni_{40}P_{19}Si_1$, one obtains the best fit to the data with $T_G^0=(518\pm6)$ K, $A=(538\pm100)$ K, and $B=(3700\pm2000)$ K/s. The best fit is shown by the solid line in Fig. 4. Equation (1) with $T_G^0=0$ is frequently used to fit similar data.[1,4–6] The extension to $T_G^0\neq0$ is somewhat *ad hoc*, however, the fits shows that the data are consistent with T_G converging to a temperature T_G^0. (Other fitting functions allow very good fits to the data as well, such as the function $T_G=T_G^0+A[\ln(\varphi/\varphi^0)]^2$, which converges at a finite heating rate φ^0. The fit to this form gives values of T_G^0 and φ^0 which lie close to the range of the data. The question of the choice of the fitting function is discussed in more detail below.) For $Pd_{40}Ni_{40}P_{19}Si_1$ and B_2O_3 Table I lists the values of the lowest T_G measured at low heating rates, $T_G^{\min}$, as well as T_G^0, T_K (based on the specific heat data by Kui and Turnbull[12]) and the temperature T_0 where the Vogel-Fulcher fit to the viscosity diverges.[9,10] T_G^0 is significantly closer to the range of the experimental data than T_0. The relatively small difference between $T_G^{\min}$ and T_G^0 indicates that the assumption of a lower limit of T_G, such as in Eq. (1), is reasonable. For the same reason, the fitted value of T_G^0 is numerically better defined than the value of T_0. For $Pd_{40}Ni_{40}P_{19}Si_1$, T_G^0 is close to the Kauzmann temperature, although the numerical coincidence most likely is accidental.

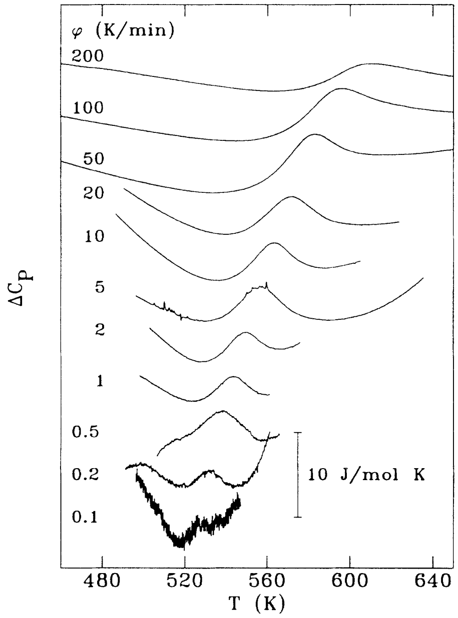

FIG. 3. Change of the specific heat at the glass transition of B_2O_3 upon heating.

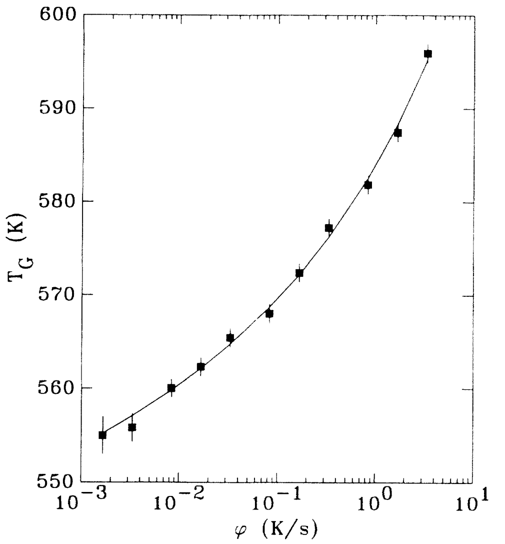

FIG. 4. Dependence of the onset of the glass transition in $Pd_{40}Ni_{40}P_{19}Si_1$ on the logarithm of the heating rate. The solid line is the best fit of the data to Eq. (1).

TABLE I. List of different temperatures (in Kelvin) which are obtained as a lower limits for T_G based on different types of measurements and extrapolations. The lowest measured value of T_G is also given.

	$Pd_{40}Ni_{40}P_{19}Si_1$	B_2O_3
$T_G^{\min}$	555±2	526±1
T_G^0 [Eq. (1)]	518±6	491±6
T_K	517±5	. . .
T^0	449±47	421±60

The data obtained for the different systems were fitted to Eq. (1) and the parameters of the best fits are given in Table II. In Fig. 5 the data are displayed together with the fits. To plot all curves in one diagram, the temperature values were scaled with the fitted values T_G^0 in Table II. Figure 5 shows that the heating rate dependences of T_G for the different systems are quite distinct with respect to the slopes and curvatures. The data for the metallic glasses $Pd_{40}Ni_{40}P_{19}Si_1$ and $Pd_{77.5}Si_{16.5}Ag_6$ are quite similar. The values of T_G for $La_{55}Al_{25}Ni_{20}$ almost follow a straight line, and as a consequence T_G^0 is much lower than $T_G^{\min}$ transition temperature. Due to the small curvature, the numerical fit of Eq. (1) to data on $La_{55}Al_{25}Ni_{20}$ and PCR is ill defined and the values for the fitted parameters have large uncertainties. B_2O_3 is the system where the deviation from a straight line is strongest. Dissolved water breaks the B–O–B bonds and thus interrupts the network structure of the glass.[15] The main effect of the difference in the water content of the two B_2O_3 samples is a change of $T_G^{\min}/T_G^0$. This indicates that on the experimental time scale, the sample with almost no dissolved water is closer to the extrapolated state formed for $T_G = T_G^0$. The two polymers behave quite similarly, and the heating rate dependence of T_G is small compared to the metallic glasses and the B_2O_3 samples.

The results suggest that for glass-forming systems an internal time scale exists. It is proportional to the parameter B in Table II, since B sets the scale for the heating rates φ. A small value of B indicates that the internal time scale of the system is short, such as for B_2O_3 and $Pd_{40}Ni_{40}P_{19}Si_1$, while a large value indicates that a long waiting time would be required to bring the system close to an ideal state (such as for $La_{55}Al_{25}Ni_{20}$). The fitted values of B indicate that the internal time scales for the systems measured here vary by at least 2 orders of magnitude.

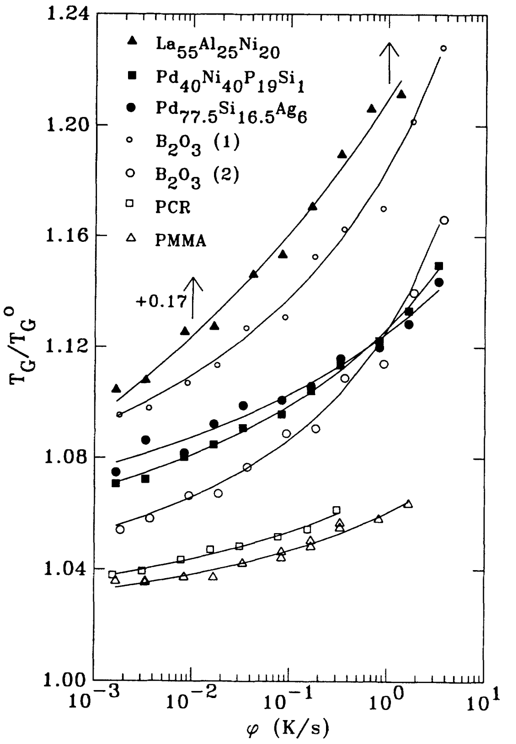

FIG. 5. Dependence of the onset of T_G on the logarithm of the heating rate. For each system T_G is scaled with the value of T_G^0 given in Table II. T_G^0 is obtained by fitting the data to Eq. (1) and the fits are shown by solid lines. The data for $La_{55}Al_{25}Ni_{20}$ are shifted down by 0.17. B_2O_3 (1) refers to the sample with less than 0.1 % H_2O and B_2O_3 (2) to the sample with 2.7 % H_2O.

TABLE II. The parameters T_G^0, A, and B for which the best fit of the data to Eq. (1) was obtained.

	T_G^0/K	A/K	$\log_{10}(B/\mathrm{K\,s^{-1}})$
Metallic glasses			
$Pd_{40}Ni_{40}P_{19}Si_1$	518±6	538±100	3.6±0.4
$Pd_{77.5}Si_{16.5}Ag_6$	576±22	770±580	4.6±2.0
$La_{55}Al_{25}Ni_{20}$	338±57	2000±2100	6.9±4.0
B_2O_3			
<0.1 mol %H_2O	491±6	310±80	2.2±0.3
2.7 mol % H_2O	439±15	550±250	2.9±0.8
Organic polymers			
PMMA	365±5	180±100	3.5±1.3
PCR	404±10	220±230	3.5±2.5

Figure 6 shows the width of the glass transition, ΔT, for the systems B_2O_3 (with less than 0.1 mol % H_2O), $Pd_{40}Ni_{40}P_{19}Si_1$, and PMMA. ΔT was taken as the difference between the temperature of the peak before the completion of the transition and the onset, as marked by the arrows in Fig. 2. For all three systems ΔT is clearly proportional to the logarithm of the heating rate over the whole experimental range. It gives an intercept with the line $\Delta T = 0$ K, which corresponds to a sharp transition. This extrapolated point of intersection gives a cooling and heating rate which lies 1–3 orders of magnitude below the lowest rates used in the present measurements. If, as this diagram suggests, the width of the glass transi-

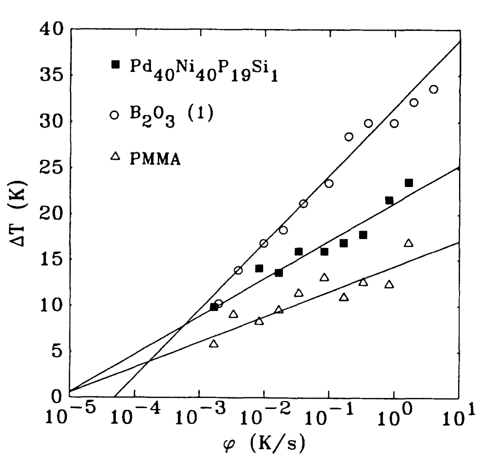

FIG. 6. Dependence of the width of the glass transition on the logarithm of the heating rate. The data for B_2O_3 refer to the sample with less than 0.1 % H_2O. The solid lines are fits to $\Delta T = a\ \ln(\varphi/\varphi^0)$ with $\varphi > \varphi^0$.

tion indeed becomes zero, or even a constant, for heating rates below a critical rate φ^0, then the glass transition is independent of the time scale of the experiment. This would be the limiting case of the transition to an ideal glass. At this point T_G would also have reached the lower limit T_G^0, since kinetic effects no longer play a role. Therefore Fig. 6 suggests that T_G may converge faster to T_G^0 than the Vogel-Fulcher form in Eq. (1), which converges only at $\varphi \rightarrow 0$. In consequence it is very likely that another fitting function, which converges for $\varphi \rightarrow \varphi^0 > 0$, may more appropriately represent a more extended range of data. Accordingly, the values given above are likely to be a lower bound of T_G^0.

CONCLUSION

Standard calorimetric measurements of the glass transition were extended to low heating and cooling rates. The previously reported results, suggesting that the relationship between T_G, or $1/T_G$, and $\ln(\varphi)$ is linear, are not valid for the extended range of data. Instead, the data are consistent with the assumption that there exists a temperature T_G^0 which is a lower limit of T_G. This lower limit lies closer to the temperature range of the experimental data than the divergence temperatures of other quantities at the glass transition, such as the correlation length or the viscosity (compare, e.g., Refs. 3, 9, and 10). T_G^0 appears to be close to Kauzmann's isentropic temperature T_K. The width of the glass transition decreases linearly with $\ln(\varphi)$. This result suggests that the width of the glass transition becomes zero, or a constant, for $\varphi < \varphi^0$. Taken together, the results indicate that shape and temperature of the glass transition may decouple from the experimental time scale for sufficiently low heating rates. In this case an ideal glass, which is independent of the thermal history, would be formed. This aspect could be of interest for the production of glasses for certain specific applications. The question remains open at this point to what the possible physical basis for a very sharp glass transition at a fixed temperature could be. It may be a strong and sudden divergence of the relaxation times at T_G^0, or it could be a thermodynamic transition, as is suggested by several models (Refs. 2, 16, and 17). Since the divergence assumed here may be tested on laboratory time scales, it is necessary and interesting to extend the measurements presented here to slower heating and cooling rates.

---

[1] J. Jäckle, Rep. Prog. Phys. **49**, 171 (1986).

[2] J. P. Sethna, J. D. Shore, and M. Huang, Phys. Rev. B **44**, 4943 (1991).

[3] E. W. Fischer, E. Donth, and W. Steffen, Phys. Rev. Lett. **68**, 2344 (1992).

[4] H. W. Gronert, F. Gillessen, and D. M. Herlach, in *Proceedings of the 6th International Conference on Rapidly Quenched Metals,* edited by R. W. Cochrane and J. O. Ström-Olsen [Mater. Sci. Eng. **97**, 191 (1988)].

[5] R. Lück, Q. Jiang, and B. Predel, J. Non-Cryst. Solids **117/118**, 911 (1990).

[6] C. T. Moynihan, A. J. Easteal, J. Wilder, and J. Tucker, J. Phys. Chem. **78**, 2673 (1974).

[7] P. K. Dixon, Phys. Rev. B **42**, 8179 (1990).

[8] A. Schönhals, F. Kremer, and E. Schlosser, Phys. Rev. Lett. **67**, 999 (1991).

[9] P. B. Macedo and A. Napolitano, J. Chem. Phys. **49**, 1887 (1968).

[10] C. A. Volkert and F. Spaepen, in *Proceedings of the 6th International Conference on Rapidly Quenched Metals,* edited by R. W. Cochrane and J. O. Ström-Olsen [Mater. Sci. Eng. **97**, 449 (1988)].

[11] W. Kauzmann, Chem. Rev. **43**, 219 (1948).

[12] H. W. Kui and D. Turnbull, J. Non-Cryst. Solids **94**, 62 (1987).

[13] J. O. Ström-Olsen, D. H. Ryan, Z. Altounian, and R. Brüning, Mater. Sci. Eng. A **133**, 403 (1991).

[14] R. Brüning, D. H. Ryan, J. O. Ström-Olsen, and L. J. Lewis, Mater. Sci. Eng. A **134**, 964 (1991).

[15] A. Feltz, *Amorphe und glasartige anorganische Festkörper* (Akademie Verlag, Berlin, 1983).

[16] J. H. Gibbs, J. Chem. Phys. **28**, 373 (1958).

[17] T. R. Kirkpatrick, D. Thirumalai, and P. G. Wolynes, Phys. Rev. A **40**, 1045 (1989).